MINERALOGICAL AND GEOCHEMICAL COMPARISON BETWEEN THE SHALES OF BEDUH AND BALUTI FORMATIONS IN THE NORTHERN THRUST ZONE, KURDISTAN REGION, IRAQ: IMPLICATION FOR PROVENANCE AND TECTONIC SETTING

Faraj H. Tobia*, Baran H. Mustafa, Sirwa S. Shangola and Mario U. Kasha

*Department of Geology, College of Science, University of Salahaddin, Erbil, Iraq
*Corresponding author: e-mail: farajabba58@gmail.com

Received: 23 May 2017; accepted: 10 August 2017

ABSTRACT

The mineralogical and geochemical data are employed to determine the provenance, paleoweathering, and depositional setting of the shales from the Beduh (L. Triassic) and Baluti (U. Triassic) formations at Sararu area N of Iraq. The mineralogical data (e.g., high illite content and moderate illite crystallinity index in Beduh shale and kaolinite in Baluti shale) and geochemical parameters of the shales (major, trace, and REE-based discrimination diagrams, Al_2O_3/TiO_2, and LREE/HREE ratios) indicate that both shales were evolved from acidic source rocks. This is reclined by the enrichment of LREEs, depletion of HREEs, and negative Eu anomaly. The paleoweathering parameters (chemical index of alteration and chemical index of weathering), in addition to the A-CN-K (Al_2O_3-CaO+Na_2O-K_2O) diagram of the Beduh shale induce that the source terrain was moderately to intensively and for Baluti shale was intensively chemically weathered. The Beduh shale was plot perpendicular to the A-K line indicates the K-metasomatism, and for Baluti shale was fall parallel to the A-K line suggesting intense weathering with no evidence for K-metasomatism. The discriminant diagrams based on major elements in addition to critical trace and REE parameters suggest that the origin of the sediments was probably from passive (Arabian Shield and the Rutba Uplift) tectonic environments for both with the effect of the active (volcanic activity) tectonism on the Beduh shale. The geochemical parameters such as U/Th, V/Cr, and Ni/Co ratios and negative Eu anomalies indicate the study shales were deposited in an oxic environment.

Keywords: Beduh Formation; Baluti Formation; REE; Shale; Provenance

INTRODUCTION

The mineralogical and geochemical data of the clastic rocks have been used to determine the degree of weathering (Fedo *et al.*, 1995; Ghandour *et al.*, 2003; Srivastava *et al.*, 2013), tectonic setting (Bhatia, 1983; Verma and Armstrong-Altrin, 2013), and the diagenesis (Zaid *et al.*, 2015), in addition it reflect the characteristics of their source rocks which some trace elements (e.g., REEs, Th, Zr, and Hf) are transformed from the site of weathering to the sedimentary basin (McLennan and Taylor, 1991; Tawfik *et al.*, 2011; Armstrong-Altrin *et al.*, 2012, 2014; Dai *et al.*, 2016). Therefore, these terrigenous materials can be preserving the characteristics of their parent rocks.

The Triassic formations in the Northern Thrust Zone in Iraq (Fig. 1) receive less attention in relative to other younger rocks. Most of the previous studies were related to structural, tectonic, and facies analyses. In 1997, Numan proposed the tectonic scenario of Iraq and suggested Beduh shale in the Werfenian, marking isolation of the Iranian Plate; and Baluti shale, marking isolation of the Turkish Plate.

The siliciclastic-dominated Beduh Formation described as 60 m thick reddish brown to reddish purple shale and marl with thin beds of limestone and hard sand (Bellen *et al.*, 1959). The shale-dominated Baluti Formation is comprised mainly of shale interbedded with thin beds of dolomitic limestones. It varies in thickness from 35 to 60 m and the age of the formation is decided by its stratigraphic position between the Upper Triassic Kurra Chine Formation and the overlying Liassic Sarki Formation (Fig. 2). However, Hanna (2007) suggested the Carnian age based on the assemblage palynozones.

The current study examines the mineralogy and geochemistry of the Beduh and Baluti shales and the objectives of this study are to compare between these shales to understand the provenance and tectonic setting of the basin during the Lower and Upper Triassic.

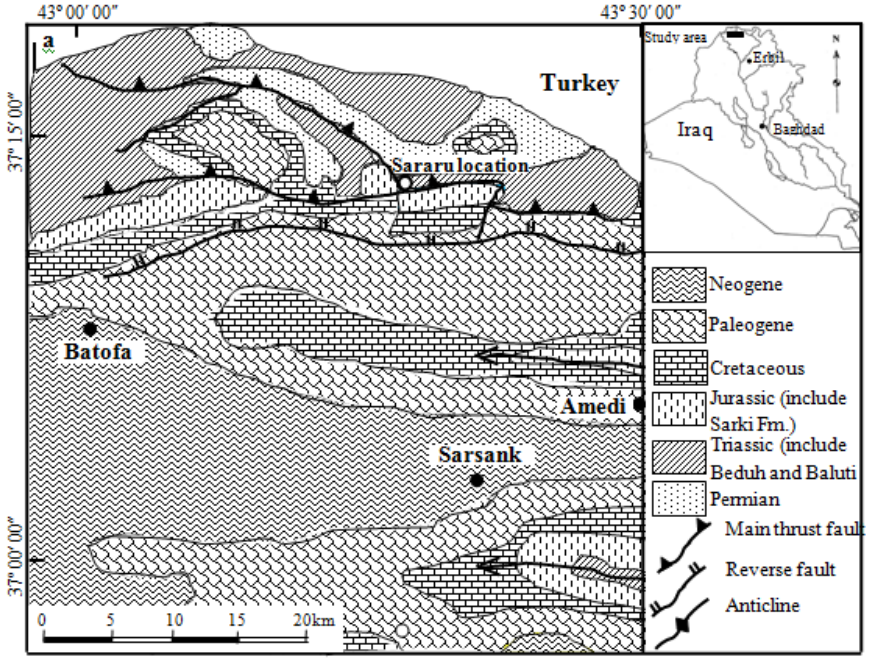

Fig. 1: Geological map and the location of the study area, (enlarged from Sissakian, 2000)

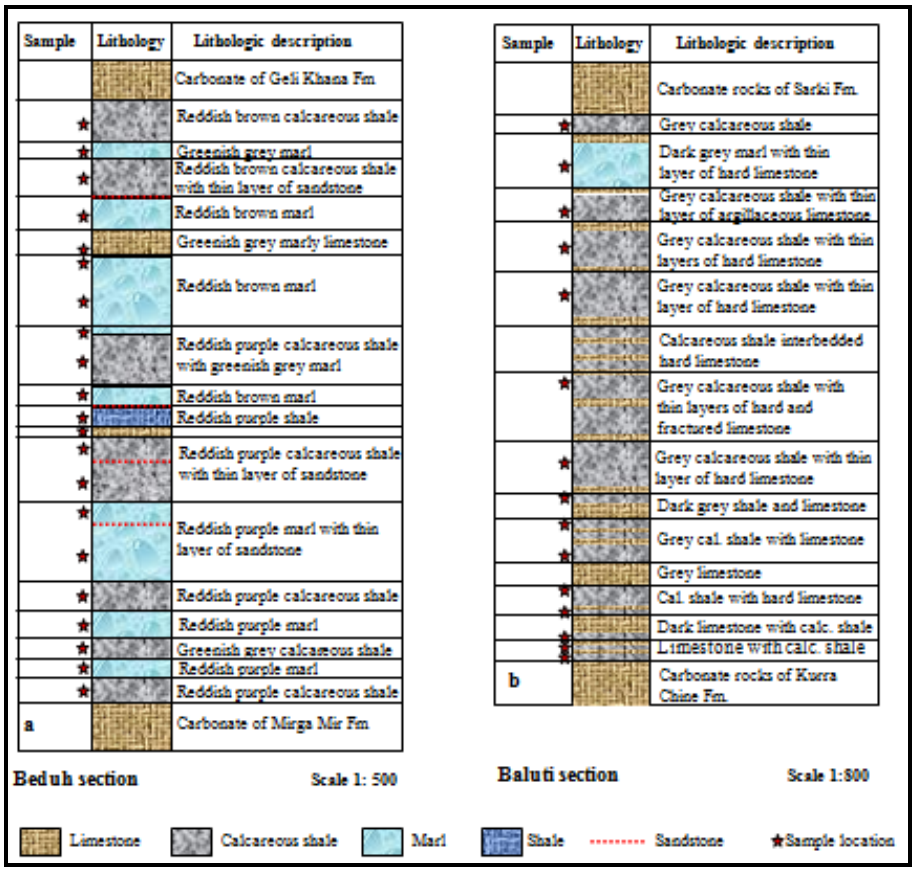

Fig. 2: Columnar sections, a) in Beduh Formation and b) in Baluti Formation, in Sararu area

GEOLOGICAL SETTING

At the Late Permian the Neo-Tethys Ocean started opening, then progressively widened during Early Triassic time (Figs. 3a and 4). The Late Permian-Liassic sequence was deposited on the north and east fringes of passive margin of the Arabian Plate. Thermal subsidence causes the formation of a passive margin sequence along these margins and the creating of the Mesopotamian Basin (Jassim *et al.*, 2006). Renewed rifting occurred within this passive margin in Mid-Late Triassic time (Fig. 3b) creating a broad and highly restricted basin in Mesopotamia splitted from the open ocean by a narrow rift with an outer ridge of thinned continental crust and development of an open marine carbonate platform (Numan, 1997; Jassim and Goff, 2006).

The Rutba Basin was gently inverted; forming the Rutba Uplift. The shoreline of the Late Permian basin was located along the eastern fault of the Rutba Uplift (Fig. 3). The Arabian Shield was composed of igneous-metamorphic complexes and was an elevated area at that time, located to the southwest of the basin of deposition.

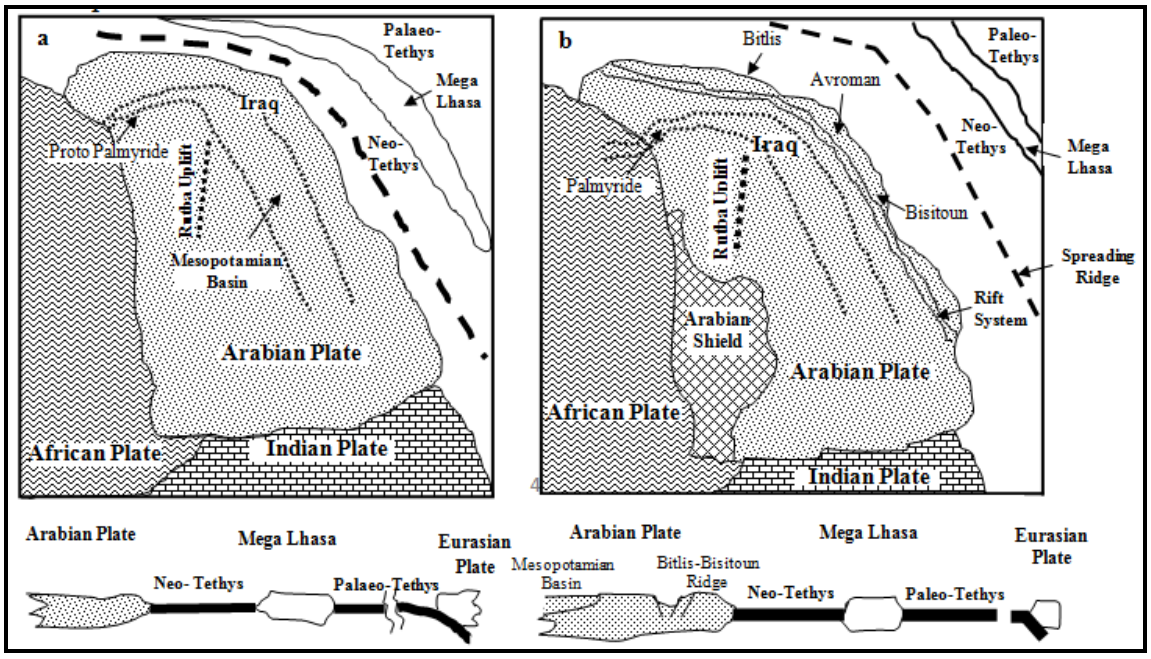

Fig. 3: a) Late Permian-Early Triassic, b) Mid Triassic-Norian geodynamic development of the Arabian Plate (after Jassim and Goff, 2006)

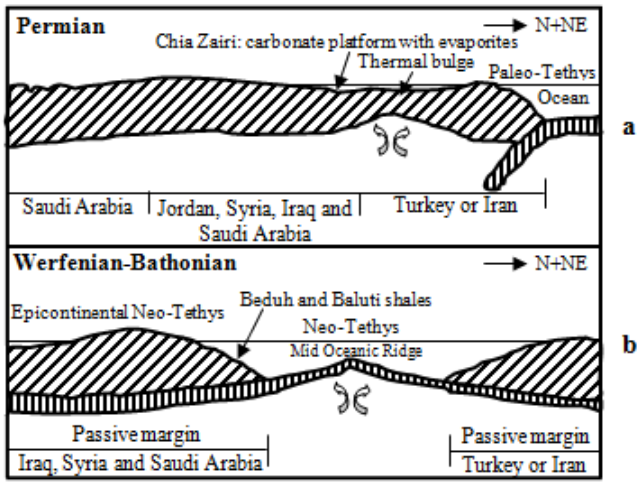

Fig. 4: Imaginary model for the Permian-Triassic plate tectonic situation of Iraq and surrounding countries: a) intraplate set-up, b) rifting set-up (after Numan, 1997)

The study area lies at 37°14′25″N and 43°18′19″E (Fig. 1). In this area, the Beduh Formation is conformably underlain by the Mirga Mir Formation and overlain by the Geli Khana Formation. The upper boundary of Baluti Formation is conformable with the Liassic Sarki Formation. Hanna (2007) suggested the Carnian (Julian) age for the upper part of Baluti Formation depending on the assemblage palynozones. He proposes the shore zone depositional environment with influence of fresh water for the lower portion of the upper part of the formation.

SAMPLING AND METHODS

Thirty six shale samples were collected from the Sararu area: 21 samples from the Beduh and sixteen samples from Baluti Formation (Fig. 2). The mineralogy of fourteen shale samples (six from Beduh and 8 from Baluti shales) was determined by conventional X-ray diffraction (XRD) method using Philips PM8203 X-ray diffractometer at the Iraqi Geological Survey Laboratories, Baghdad, Iraq. The oriented clay samples were run under three different conditions: air-dried state, ethylene glycolation at 25 °C for 15 h, and after heating to 550°C for 1 h. The area under curve of specific reflections of the clay minerals was calculated for the semiquantitative analysis (Carroll, 1970).

The 36 shale samples were analyzed for major, trace, and rare earth elements. Chemical analyses of Beduh shale were performed at Acme Analytical Laboratories, Vancouver, Canada; and for Baluti shale at ALS international laboratory in Spain. The

major element contents were analyzed by X-ray fluorescence spectrometry, Loss on ignition (LOI) was calculated after ignition at 1000 °C for 2 h. Trace and REE concentrations were measured by inductively coupled plasma mass spectrometer. Chemical analysis for major elements has precisions up to 3 %; whereas it varies from 1 to 10% for the trace and REEs.

Based on the standards, the accuracy and the precision of the analyses were within ±2% to ±10%. The Post-Archean Australian shale (PAAS) values were used for comparison. The REE data were normalized to the chondrite values of Taylor and McLennan (1985). The normalized Eu anomaly (Eu/Eu*) was calculated by the following equation: $Eu/Eu^* = Eu_n/(Sm_n \times Gd_n)^{1/2}$, where the subscript n denotes chondrite normalized values (Taylor and McLennan, 1985). CaO was corrected by the method of McLennan *et al*. (1993).

RESULTS

Mineralogy

XRD analysis of selected Beduh shale samples indicates that clay minerals are mainly represented by illite and kaolinite, with small amounts of chlorite and a mixed layer (illite/smectite and illite/chlorite). On the other hand, calcites and quartz together with minor amounts of albitic feldspar and hematite are the dominant non-clay species (Fig. 5a). The analysis revealed qualitative differences in bulk mineral compositions (Table 1). Illite and kaolinite have an average of 58.07% and 26.05%, respectively. The samples generally showed moderate illite crystallinity index with an average of 0.49° Δ2θ (Table 1). All the study shales have illite chemistry index (5A°/10A° ratios) of >0.4 (Table 1).

However, the Baluti shales are mainly comprised of clay minerals with calcite, quartz, and minor amounts of muscovite; and the main clay minerals are kaolinite, illite, and mixed layer illite/smectite (Fig. 5b). Illite and kaolinite have an average 32.9% and 32.3%, respectively. The average of Kübler illite index is1.0 Δ2θ (Table 1); the modal illite crystallinity value is 0.69 Δ2θ which is typical for a high diagenetic zone (Merriman and Frey, 1999). The average of illite chemistry index is 0.59 and kaolinite crystallinity index is 0.15.

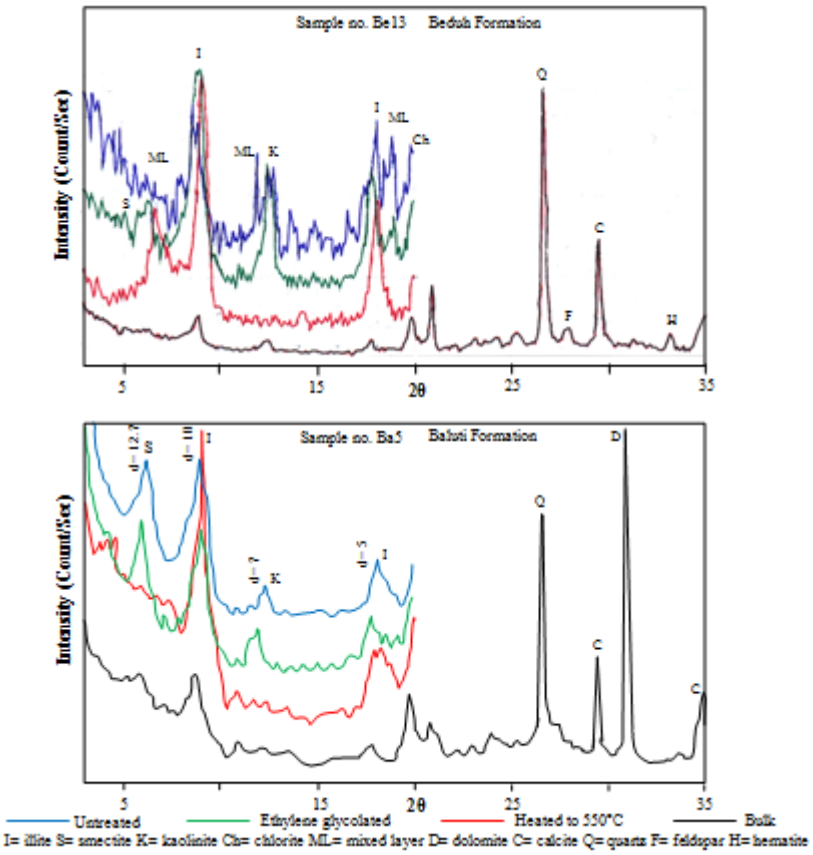

Fig. 5: X-ray diffractograms for selected shale samples from, a) Beduh Formation and b) Baluti Formation

Table 1: Mineralogical composition and crystallographic parameters for the shales from Beduh and Baluti formations

	Non-clay minerals					Clay minerals						
	Calcite %	Quartz %	Feldspar %	Muscovite %	Hematite %	Illite %	Kaolinite %	Chlorite %	Mixed layer %	Illite chemistry index	Illite crystallinity index (2θ)	Kaolinite crystallinity index
	Beduh shale											
Be4	64.9	29.6	3.2	2.3	-	52.4	34.1	13.5		0.51	0.42	0.03
Be5	50.9	40.8	3.8	3.1	1.4	57.2	19.3		23.5[1]	0.59	0.50	0.04
Be13	29.8	59.0	2.0	6.6	2.6	53.4	24.0		22.6[1]	0.92	0.52	0.08
Be19	65.0	28.6	4.8	1.6	-	57.8	28.9	13.3		0.44	0.58	0.03
Be20	85.0	13.1	1.4	0.5	-	50.1	44.1	5.8		0.64	0.52	0.04
Be25	30.9	60.9	1.4	4.3	2.5	77.5	5.9		16.6[2]	0.52	0.41	0.21
average	54.42	38.67	2.77	3.07	2.17	58.07	26.05	10.87	20.91	0.60	0.49	0.07
	Baluti shale											
Ba1	91.45	7.43	-	1.12	-	51.8	10.7	-	37.5[2]	0.88	0.8	0.15
Ba3	89.3	10.7	-	----	-	27.0	46.0	-	27.0[2]	0.58	1.2	0.05
Ba5	95.1	4.9	-	----	-	30.7	41.8	-	27.5[2]	0.85	1.0	0.05
Ba7	95.1	4.9	-	----	-	29.4	44.5	-	26.1[2]	0.58	1.2	0.04
Ba9	94.25	4.89	-	0.86	-	30.6	38.8	-	30.6[2]	0.13	0.8	0.03
Ba11	91.92	6.73	-	1.35	-	30.8	54.4	-	14.8[2]	0.51	1.0	0.05
Ba13	91.27	6.72	-	2.01	-	57.6	6.9	-	35.5[2]	0.72	1.2	0.72
Ba15	92.96	5.63	-	1.41	-	35.9	14.9	-	49.2[2]	0.45	0.8	0.13
average	92.67	6.4	-	1.35	-	32.9	32.3	-	31.0	0.59	1.0	0.15

Major element geochemistry

The major element concentrations of the Beduh and Baluti shales are given in Table 2. Both shales have high CaO content. Such content has a great dilution effect on the other oxides. The average of SiO_2 content in the Beduh is 36.38%, and 9.12 % in Baluti shale. Al_2O_3 content is 11.37% in Beduh and 14.60% in the Baluti. The TiO_2 content of both shales is relatively low (0.46% in Beduh and 0.48% in Baluti). The average of K_2O content is 3.68% for Beduh and 5.64% for Baluti shales. Na_2O content is 0.61% for Beduh and 0.09% for Baluti shales. Except for CaO, the study shales show depletion in all elements relative to those of the PAAS (Table 2).

Table 2: Major oxides concentrations (wt %) for the shales from the Beduh and Baluti formations; compared with PAAS and UCC (Taylor and McLennan, 1985)

		SiO_2	Al_2O_3	Fe_2O_3	CaO	MgO	Na_2O	K_2O	MnO	TiO_2	P_2O_5	LOI
Beduh Formation	Be1	51.05	17.33	6.50	7.39	2.09	0.65	4.26	0.05	0.64	0.12	10.29
	Be2	33.66	10.05	3.68	25.20	1.43	0.73	2.14	0.06	0.44	0.08	22.52
	Be3	46.82	14.27	6.19	12.21	2.10	0.88	3.21	0.05	0.56	0.11	13.30
	Be4	32.41	10.35	3.60	25.63	1.52	0.62	2.19	0.05	0.41	0.08	22.91
	Be5	40.93	13.59	5.19	17.09	1.74	0.57	3.23	0.04	0.51	0.11	16.96
	Be6	28.42	8.00	2.85	30.66	1.21	0.62	1.62	0.06	0.35	0.07	26.21
	Be7	33.13	11.51	4.07	23.93	1.48	0.49	2.64	0.05	0.43	0.07	22.09
	Be8	47.52	13.79	5.20	13.28	1.89	0.77	3.18	0.06	0.54	0.10	14.05
	Be9	40.32	12.78	5.47	17.93	1.85	0.66	3.01	0.05	0.51	0.10	17.52
	Be10	21.61	6.50	2.34	35.48	1.07	0.51	1.32	0.06	0.27	0.05	30.05
	Be11	49.59	17.52	7.08	7.48	2.20	0.56	4.30	0.04	0.62	0.12	10.36
	Be12	24.28	7.52	2.52	33.46	1.16	0.50	1.53	0.05	0.32	0.06	28.46
	Be13	37.88	13.18	5.57	19.19	1.73	0.47	3.19	0.04	0.50	0.10	18.77
	Be14	28.22	5.80	1.95	32.70	1.07	0.65	1.07	0.07	0.30	0.09	27.67
	Be15	32.51	11.18	4.28	24.42	1.50	0.47	2.55	0.04	0.45	0.10	22.46
	Be16	29.05	7.96	3.02	29.98	1.24	0.75	1.62	0.05	0.39	0.11	25.63
	Be17	19.46	5.99	2.01	38.13	1.19	0.42	1.15	0.05	0.29	0.07	31.53
	Be18	26.15	8.33	3.21	31.31	1.23	0.45	1.81	0.05	0.35	0.08	27.16
	Be19	41.28	13.44	5.39	16.80	1.68	0.46	3.23	0.04	0.52	0.12	17.16
	Be20	24.34	6.96	2.43	34.02	1.13	0.54	1.42	0.04	0.32	0.07	28.87
	Be21	46.43	16.59	6.97	9.99	1.89	0.29	4.14	0.04	0.62	0.12	12.97
	Average	35.00	11.08	4.26	23.16	1.54	0.57	2.51	0.05	0.44	0.09	21.28
Baluti Formation	Ba1	10.37	12.82	4.29	35.70	0.96	0.08	3.23	0.01	0.43	0.18	31.80
	Ba2	8.48	14.21	4.86	35.42	0.86	0.08	2.94	0.01	0.46	0.18	32.00
	Ba3	18.38	12.82	6.98	28.84	0.66	0.11	3.78	0.02	0.72	0.21	27.40
	Ba4	10.27	17.98	6.35	31.08	0.65	0.08	2.89	0.02	0.59	0.21	29.80
	Ba5	6.45	11.99	6.44	36.68	1.29	0.08	2.22	0.02	0.40	0.22	33.60
	Ba6	11.40	23.94	5.98	25.97	0.81	0.11	3.74	0.02	0.79	0.18	27.00
	Ba7	6.48	14.78	5.18	36.40	0.60	0.08	2.63	0.02	0.46	0.21	33.00
	Ba8	11.17	13.99	5.49	17.36	12.27	0.16	6.10	0.04	0.36	0.15	32.80
	Ba9	8.06	12.03	5.38	36.96	0.63	0.08	2.27	0.02	0.38	0.22	33.60
	Ba10	4.86	11.20	7.12	38.36	0.70	0.08	2.77	0.02	0.37	0.22	33.20
	Ba11	9.33	17.95	5.29	32.06	0.50	0.08	2.75	0.02	0.56	0.22	31.00
	Ba12	5.14	14.93	4.92	36.68	0.68	0.08	3.42	0.02	0.47	0.26	32.20
	Ba13	8.55	15.76	5.12	33.60	0.76	0.08	3.93	0.02	0.50	0.23	31.40
	Ba14	5.95	9.95	5.58	38.92	1.08	0.08	2.60	0.01	0.30	0.22	33.20
	Ba15	11.55	14.67	5.69	32.34	0.75	0.08	3.11	0.01	0.47	0.23	31.00
	Average	9.12	14.60	5.64	33.09	1.55	0.09	3.23	0.02	0.48	0.21	31.53
PAAS		62.40	18.78	7.18	1.29	2.19	1.19	3.68	0.11	0.99	0.16	6.00

Trace element geochemistry

The trace element concentrations of the Beduh and Baluti shales are reported in Table 3. The study shales show enrichment in Sr, Ba, and Th; and depletion in Rb, U, Y, Zr, Nb, Hf, V, Cr, Co, Ni, Cu and Zn relative to PAAS (Table 3). The high concentration of Sr (average = 418 ppm) in a few samples is probably linked to the carbonate content (Yan *et al*., 2007). This is conform to the significant positive correlation between CaO and Sr (r = 0.871) in Beduh and (r = 0.820) in Baluti. Al_2O_3 is positively correlated with HFSEs such as Y, Zr, Nb, and Hf (for Beduh, r = 0.741, 0.586, 0.934, and 0.579; and for Baluti, r = 0.671, 0.525, 0.632, and 0.725) and LILEs such as Th (r = 0.908 for Beduh and 0.737 for Baluti); and to TTEs such as V, Co, and Ni (for Beduh, r = 0.969, 0.932, and 0.964; and for Baluti, r = 0.650, 0.813, and 0.552), suggesting their incorporation in clay fractions and concentrated during weathering (Fedo *et al.*, 1996; Nagarajan *et al.*, 2007) and some of them (such as Zr and Hf) are associated with the heavy minerals.

Table 3: Trace element concentrations (ppm) for the shales from the Beduh and Baluti formations, compared with PAAS and UCC (Taylor and McLennan, 1985)

		Large ion lithophile elements					High field strength elements				Transition elements					
		Rb	Sr	Ba	Th	U	Y	Zr	Nb	Hf	V	Cr	Co	Ni	Cu	Zn
Beduh Formation	Be1	149.0	184.2	321	17.5	3.8	26.0	117.9	11.8	3.4	103	47.9	14.0	29.2	7.9	82
	Be2	79.7	502.8	222	10.4	3.1	19.4	100.8	8.9	2.6	65	34.2	9.1	17.3	12.2	44
	Be3	126.5	243.9	276	13.7	2.7	28.9	116.4	12.0	3.3	81	41.0	14.1	28.2	20.9	81
	Be4	83.7	540.2	350	10.2	3.1	17.0	84.5	8.1	2.2	69	34.2	9.2	20.3	17.8	53
	Be5	127.3	372.2	239	11.0	2.6	22.6	117.9	10.2	3.1	82	27.4	11.3	24.3	28.4	63
	Be6	57.2	774.4	556	7.2	2.4	15.5	93.4	6.2	2.8	52	37.6	7.2	14.9	3.1	41
	Be7	101.6	529.8	223	8.6	2.7	17.2	84.3	8.5	2.4	73	41.0	9.6	18.2	32.2	54
	Be8	131.7	219.5	212	11.4	2.5	21.9	130.6	13.1	3.8	83	44.5	12.4	23.0	21.2	64
	Be9	120.2	295.5	226	12.3	2.7	23.2	106.6	11.1	2.8	77	41.0	11.6	22.1	2.9	59
	Be10	55.3	894.4	113	6.1	2.1	14.1	60.7	5.8	1.8	35	23.9	7.1	10.4	8.6	36
	Be11	174.8	201.1	297	15.2	2.9	26.9	127.0	12.9	3.7	98	41.0	15.5	28.0	10.8	82
	Be12	71.1	1012.	148	6.5	2.3	14.9	72.1	6.8	1.9	43	27.4	7.8	12.0	13.0	41
	Be13	126.8	353.4	220	11.7	2.4	20.5	100.0	9.7	3.0	71	34.2	10.8	22.3	2.0	60
	Be14	42.8	469.2	263	7.1	2.7	15.4	91.3	5.9	2.7	28	23.9	5.8	11.5	71.1	30
	Be15	110.1	495.2	277	11.5	2.8	21.6	94.4	9.2	2.8	71	37.6	10.9	19.5	13.4	53
	Be16	68.4	492.0	405	10.9	3.3	23.6	88.2	8.1	2.1	43	23.9	7.8	14.7	1.2	41
	Be17	51.4	629.4	334	8.0	2.7	16.9	60.6	6.0	1.8	29	20.5	6.4	12.0	32.6	33
	Be18	76.2	655.1	146	8.4	2.3	17.1	79.8	7.4	2.0	49	27.4	7.9	15.9	10.9	41
	Be19	124.2	282.2	243	12.1	3.5	21.4	104.6	9.9	2.8	73	68.4	12.4	27.7	8.3	71
	Be20	59.7	811.5	164	7.0	2.4	14.0	81.5	6.7	2.3	34	27.4	6.9	14.2	8.0	39
	Be21	163.7	199.1	298	15.0	3.6	27.1	125.4	12.5	3.4	104	44.5	14.5	31.7	11.1	79
	Avera	100.0	483.6	263.	10.56	2.79	20.25	97.05	9.09	2.70	64.9	35.6	10.1	19.88	16.0	54.6
Baluti Formation	Ba1	33.7	497	40	5.7	2.3	14.9	74.2	10.7	2.1	100	54	6.3	39.5	9.3	48
	Ba2	35.3	449	50	6.2	3.1	15.9	76.7	11.4	2.1	112	51	7.2	41.5	10.5	15
	Ba3	47.1	495	60	9.0	3.0	20.9	149.0	17.8	3.2	175	70	9.5	58.3	15.4	78
	Ba4	36.3	527	50	7.8	3.1	18.9	102.0	14.3	2.7	150	59	8.3	52.8	13.4	89
	Ba5	28.2	696	40	5.2	2.6	15.4	65.7	9.9	1.8	98	78	6.4	43.0	34.4	66
	Ba6	52.1	409	60	9.5	3.4	21.0	133.0	19.7	3.5	182	99	13.6	67.6	38.3	108
	Ba7	33.3	653	40	5.8	2.7	14.7	71.1	11.5	2.0	115	57	6.4	48.2	12.7	45
	Ba8	64.5	110	60	4.4	3.6	13.9	121.5	19.8	2.9	48	32	5.8	17.6	15.2	24
	Ba9	27.6	611	30	5.0	2.8	12.5	63.7	9.3	1.7	111	50	5.3	42.1	12.5	15
	Ba10	25.3	516	30	4.8	2.6	12.3	62.1	8.4	1.7	99	51	5.1	39.0	15.1	12
	Ba11	33.4	404	40	6.9	2.9	15.4	85.0	12.9	2.4	149	63	7.3	42.0	11.3	44
	Ba12	33.2	545	40	5.8	3.0	14.1	69.4	11.1	2.1	123	53	6.5	50.6	13.8	16
	Ba13	36.7	360	40	6.7	3.4	16.7	86.5	12.3	2.3	139	56	10.0	52.8	15.0	58
	Ba14	25.4	604	40	4.4	2.8	11.6	54.8	7.3	1.3	91	44	4.5	41.3	13.2	81
	Ba15	32.7	475	40	6.1	3.5	13.9	72.4	11.2	2.1	123	55	5.8	46.2	11.4	56
	Avera	36.3	490	44	6.2	2.9	15.4	85.8	12.5	2.2	100	58.1	7.2	45.5	16.1	50.3
PAAS		650	23	15	5	19	160	200	14.6	3.1	150	210	27	50	20	85

The average of total rare earth elements (ΣREE) is 146.40 ppm for Beduh shale, and 117.17 ppm for Baluti shale; both are lower than for the PAAS (184.77 ppm; Table 4). The results show the dilution effect caused by carbonate, is a major control over the REE concentrations (correlation coefficient between CaO and ΣREE is -0.875 for Beduh and -0.348 for Baluti). In this regard, the significant correlations of ΣREE with Al_2O_3 and TiO_2 (for Beduh, r = 0.870 and 0.899, and for Baluti r = 0.672 and 0.955, respectively) suggest that clay minerals typically control REE distribution in the shales (McLennan, 1989; Condie, 1991). The chondrite normalized (Taylor and McLennan, 1985) REE patterns of these shales (Fig. 6) exhibit LREE enrichment and negative Eu anomaly (Eu/Eu* = 0.73 for Beduh and 0.68 for Baluti).

Table 4: REE concentrations (ppm) for the shales from the Beduh and Baluti formations

		La	Ce	Pr	Nd	Sm	Eu	Gd	Tb	Dy	Ho	Er	Tm	Yb	Lu	SUM
Beduh Formation	Be1	44.2	87.2	10.09	36.4	6.07	1.06	4.78	0.88	4.73	0.98	2.67	0.40	2.47	0.37	202.30
	Be2	26.7	53.9	6.09	21.1	4.05	0.73	3.17	0.66	3.51	0.72	1.83	0.26	1.57	0.25	124.54
	Be3	40.8	81.9	8.66	31.6	5.44	1.13	5.77	0.89	4.40	0.87	2.52	0.36	2.50	0.41	187.25
	Be4	26.4	52.4	6.11	21.8	4.26	0.76	3.22	0.62	2.93	0.60	1.64	0.24	1.66	0.23	122.87
	Be5	29.8	60.4	6.85	25.7	5.06	0.99	4.29	0.65	3.49	0.74	2.09	0.33	2.12	0.33	142.84
	Be6	21.3	43.6	4.64	15.6	3.14	0.59	3.34	0.51	2.42	0.48	1.19	0.18	1.18	0.19	98.36
	Be7	24.4	47.7	5.20	18.5	3.57	0.73	3.58	0.52	2.39	0.52	1.54	0.22	1.62	0.25	110.74
	Be8	31.9	62.1	7.53	29.5	5.85	1.14	5.04	0.68	4.25	0.87	2.31	0.39	2.48	0.35	154.39
	Be9	33.1	66.4	8.15	31.9	6.56	1.26	4.83	0.74	4.65	0.89	2.50	0.36	2.33	0.35	164.02
	Be10	18.6	36.9	4.52	17.1	3.64	0.70	2.96	0.43	2.62	0.53	1.47	0.19	1.38	0.18	91.22
	Be11	41.3	80.2	9.62	35.6	6.32	1.26	5.44	0.79	4.90	0.94	2.93	0.41	2.97	0.42	193.10
	Be12	20.0	38.5	4.86	19.6	3.95	0.79	3.39	0.44	2.75	0.49	1.46	0.24	1.49	0.21	98.17
	Be13	33.4	65.8	8.03	30.4	5.65	1.05	4.00	0.64	4.32	0.78	2.28	0.32	1.97	0.32	158.96
	Be14	20.7	41.4	5.28	20.6	4.39	0.88	3.66	0.54	3.08	0.56	1.67	0.21	1.45	0.22	104.64
	Be15	32.8	63.8	7.59	27.8	5.64	1.16	4.43	0.66	4.09	0.74	2.13	0.33	2.12	0.32	153.61
	Be16	32.9	67.1	7.89	31.7	6.33	1.14	5.14	0.75	5.07	0.89	2.51	0.37	2.43	0.32	164.54
	Be17	24.1	48.5	6.09	24.0	5.01	0.94	3.60	0.54	3.51	0.59	1.80	0.26	1.57	0.24	120.75
	Be18	25.6	48.7	6.05	23.5	5.01	0.90	3.49	0.55	3.45	0.63	1.82	0.25	1.72	0.27	121.94
	Be19	36.5	73.0	8.74	31.9	5.98	1.07	4.24	0.69	4.35	0.76	2.21	0.35	2.21	0.37	172.37
	Be20	19.5	36.9	4.36	17.3	3.36	0.67	3.05	0.41	2.70	0.46	1.35	0.20	1.40	0.21	91.87
	Be21	43.7	86.1	10.23	39.7	7.14	1.30	5.38	0.88	5.44	0.99	2.96	0.44	2.78	0.44	207.48
	Average	29.89	59.17	6.98	26.25	5.07	0.96	4.13	0.64	3.76	0.72	2.04	0.30	1.97	0.30	142.19
Baluti Formation	Ba1	22.60	52.60	5.65	22.10	4.16	0.77	3.24	0.51	2.92	0.54	1.57	0.22	1.41	0.22	118.51
	Ba2	23.80	52.00	5.94	23.50	4.31	0.85	3.41	0.55	3.16	0.59	1.67	0.23	1.51	0.23	121.75
	Ba3	35.10	69.80	8.08	29.90	5.59	1.10	4.58	0.70	4.05	0.75	2.28	0.33	2.13	0.33	164.72
	Ba4	29.70	60.10	6.85	27.10	4.96	1.02	4.09	0.66	3.79	0.70	2.03	0.29	1.86	0.29	143.44
	Ba5	21.60	48.10	5.46	21.50	4.12	0.80	3.24	0.49	2.77	0.51	1.46	0.21	1.32	0.21	111.79
	Ba6	35.50	71.80	8.10	30.90	5.55	1.09	4.33	0.72	4.19	0.80	2.39	0.33	2.26	0.33	168.29
	Ba7	22.20	48.80	5.38	20.60	3.76	0.79	3.19	0.48	2.79	0.51	1.51	0.21	1.37	0.22	111.81
	Ba8	18.70	39.00	4.56	16.70	3.02	0.58	2.73	0.45	2.70	0.52	1.58	0.22	1.43	0.23	92.42
	Ba9	19.10	38.40	4.50	17.70	3.29	0.65	2.61	0.40	2.29	0.45	1.28	0.18	1.10	0.18	92.13
	Ba10	18.60	39.50	4.53	17.70	3.21	0.67	2.69	0.42	2.36	0.46	1.34	0.18	1.13	0.19	92.98
	Ba11	24.40	49.70	5.75	21.70	4.06	0.85	3.41	0.53	3.09	0.58	1.67	0.24	1.56	0.24	117.78
	Ba12	21.50	45.40	5.19	20.20	3.78	0.75	3.12	0.47	2.80	0.51	1.49	0.22	1.38	0.22	107.03
	Ba13	24.90	51.50	5.99	23.90	4.37	0.90	3.89	0.59	3.41	0.62	1.79	0.25	1.60	0.25	123.96
	Ba14	17.00	35.10	4.23	16.80	3.14	0.61	2.48	0.38	2.18	0.41	1.17	0.16	1.04	0.16	84.86
	Ba15	21.80	44.20	5.24	20.00	3.82	0.79	3.08	0.50	2.80	0.53	1.52	0.22	1.34	0.22	106.06
	Average	23.77	49.73	5.70	22.02	4.08	0.81	3.34	0.52	3.02	0.57	1.65	0.23	1.50	0.23	117.17
PAAS		38.2	79.6	8.83	33.9	5.55	1.08	4.66	0.77	4.68	0.99	2.85	0.41	2.82	0.43	184.77

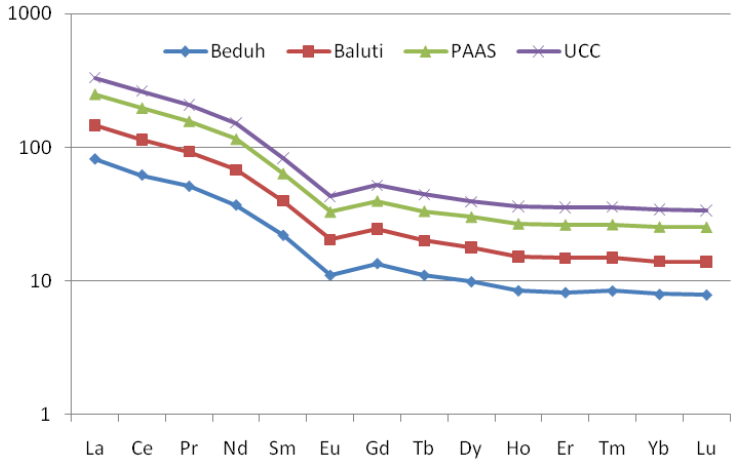

Fig. 6: Chondrite normalized rare earth elements plot for the shale samples of Beduh and Baluti compared with PAAS and UCC; Chondrite normalization values are from Taylor and McLennan (1985)

DISCUSSION

Clay mineralogy

The moderate illite crystallinity index values indicate a moderate-grade chemical degradation in the source area during transportation and sedimentation. According to the illite crystallinity index most of the studied samples plotted in the zone of diagenesis. Both study shales have an illite chemistry index value of >0.4 (Table 1), corresponding Al-rich illite (muscovite type) reflecting a granitic provenance. The kaolinite has a low crystallinity index, i.e. high crystallinity, which can be explained by being directly supplied from the rivers (Oliveira *et al.*, 2002). Kaolinite has been accepted for a long time as a product of chemical weathering. Kaolinite formation is, therefore, favored under tropical to subtropical humid climatic conditions (Chamley, 1989; Hallam *et al.*, 1991). Kaolinite may also formed by diagenetic processes indicated by the Al-shale enrichment of the Baluti Formation. Illite is developing in soils with low chemical weathering in cold and/or dry climates, and in areas of high relief where physical erosion is common. Kaolinite was concentrate in sediments of non-marine conditions and marginal marine settings, whereas smectite is proposed to have higher contents in normal marine shales. This could be attributed to the hydraulic separation of clay minerals (Raucsik and Merényi, 2000). Accordingly, it may suggest that the shales of Beduh and Baluti were developed under tropical to subtropical climate.

Source area weathering

The rate of chemical weathering of source rocks and the erosion of the profiles are controlled by climate in addition to the composition of the source rock and tectonics; warm humid climate and stable tectonic settings favor chemical weathering. Absent of chemical alteration results in low CIA values, which may reflect cool and/ or arid conditions or alternatively rapid physical weathering and erosion under an active tectonic setting (Fedo *et al.*, 1995; Nesbitt *et al.*, 1997; Absar and Sreenivas, 2015; Tawfik *et al.*, 2015). Different source materials have different initial CIA values. For example, basalts have a CIA of <45 (Sheldon, 2003), felsic rocks 55 – 60, and shales 70 – 75 (Nesbitt and Young, 1982; Maynard, 1992), indicating a moderate to high degree of chemical weathering. The degree of weathering in clastic sediments at the source area can be estimated by the relationships between alkali and alkaline earth elements (Nesbitt and Young, 1996; Nesbitt *et al.*, 1997). This can be deduced through the calculated values of the CIA, CIW, and ICV which are defined as follows:

$CIA= [Al_2O_3 / (Al_2O_3+CaO^*+Na_2O+K_2O)] x100$ (Nesbitt and Young, 1982)

$CIW= [Al_2O_3 / (Al_2O_3+CaO^*+Na_2O)] x 100$ (Harnois, 1988)

$ICV= (CaO+ K_2O+ Na_2O+ Fe_2O_3+ MgO+ MnO+ TiO_2)/Al_2O_3$ (Cox *et al.*, 1995)

where the oxides are expressed as molar proportions and CaO* represent the Ca in silicate fractions only.

The CIA values of the study shales vary from 71.76 to 76.24 (average = 74.32) in the Beduh and from 67.03 to 85.21 (average = 79.82) in the Baluti (Table 5). The former average is nearly similar to PAAS (=75; Taylor and McLennan, 1985) and the latter is higher; this implies that the sediments of Beduh suffered moderate to high degree of weathering and for Baluti are subjected to intense degree of weathering. The CIA values are also plotted on the Al_2O_3- (CaO^*+Na_2O)- K_2O (A-CN-K) diagram (Fig. 7) to evaluate the extent of weathering in the igneous rocks (Nesbitt and Young, 1984) and K-metasomatism (Fedo *et al.*, 1995).

Figure 7 show the Beduh shale forms a weathering trend that is almost perpendicular to the A-K line close to the illite composition, suggesting K-enrichment during diagenesis. The Beduh shale shows a deflection trend from the predicted weathering trend and the pre-metasomatism CIA values of the shales range between 72.5 and 88.0 with an average of 80.25. However, the study samples of Baluti fall parallel and along the A-K line close to illite field suggesting high degree of chemical weathering with no clear evidence of K-metasomatism.

Table 5: Paleoweathering parameters and REE ratios for the shales from Beduh and Baluti formations

		CIA	CIW	ICV	LREE	HREE	LREE/HREE	ΣREE	Eu/Eu*	$(La/Yb)_{CN}$	$(La/Sm)_{CN}$
Beduh Formation	Be1	74.61	94.19	0.99	183.96	18.34	10.03	202.30	0.68	10.07	4.58
	Be2	73.48	89.33	1.13	111.84	12.7	8.81	124.54	0.70	9.57	4.15
	Be3	73.72	90.79	1.15	168.4	18.85	8.93	187.25	0.70	9.18	4.72
	Be4	74.72	91.03	1.08	110.97	11.9	9.33	122.87	0.71	8.95	3.90
	Be5	74.72	93.55	1.02	127.81	15.03	8.50	142.84	0.73	7.91	3.71
	Be6	73.69	88.69	1.15	88.28	10.08	8.76	98.36	0.63	10.15	4.27
	Be7	75.19	93.45	0.99	99.37	11.37	8.74	110.74	0.70	8.47	4.30
	Be8	73.90	91.59	1.08	136.88	17.51	7.82	154.39	0.72	7.24	3.43
	Be9	73.97	92.17	1.12	146.11	17.91	8.16	164.02	0.77	7.99	3.18
	Be10	73.57	88.57	1.19	80.76	10.46	7.72	91.22	0.74	7.58	3.22
	Be11	75.15	95.00	1.00	173.04	20.06	8.63	193.10	0.74	7.82	4.11
	Be12	74.63	90.14	1.11	86.91	11.26	7.72	98.17	0.74	7.55	3.19
	Be13	75.02	94.46	1.03	143.28	15.68	9.14	158.96	0.76	9.54	3.72
	Be14	71.76	84.43	1.33	92.37	12.27	7.53	104.64	0.76	8.03	2.97
	Be15	75.32	93.53	1.03	137.63	15.98	8.61	153.61	0.80	8.70	3.66
	Be16	72.17	86.58	1.24	145.92	18.62	7.84	164.54	0.69	7.62	3.27
	Be17	75.02	89.66	1.23	107.7	13.05	8.25	120.75	0.76	8.64	3.03
	Be18	74.90	91.84	1.10	108.86	13.08	8.32	121.94	0.74	8.37	3.22
	Be19	75.26	94.67	1.00	156.12	16.25	9.61	172.37	0.73	9.29	3.84
	Be20	73.59	88.68	1.18	81.42	10.45	7.79	91.87	0.72	7.84	3.65
	Be21	76.24	97.20	0.94	186.87	20.61	9.07	207.48	0.72	8.84	3.85
	Average	74.32	91.41	1.07	127.36	14.83	8.54	142.19	0.73	8.54	3.71
Baluti Formation	Ba1	77.90	98.98	0.74	107.11	11.4	9.40	118.51	0.64	10.83	3.42
	Ba2	81.05	99.08	0.66	109.55	12.2	8.98	121.75	0.68	10.65	3.48
	Ba3	74.96	98.61	0.90	148.47	16.25	9.14	164.72	0.66	11.14	3.95
	Ba4	84.62	99.27	0.55	128.71	14.73	8.74	143.44	0.69	10.79	3.77
	Ba5	82.52	98.91	0.88	100.78	11.01	9.15	111.79	0.67	11.06	3.30
	Ba6	84.96	99.25	0.47	151.85	16.44	9.24	168.29	0.68	10.61	4.03
	Ba7	83.20	99.12	0.58	100.74	11.07	9.10	111.81	0.70	10.95	3.72
	Ba8	67.03	98.15	3.03	81.98	10.44	7.85	92.42	0.62	8.84	3.90
	Ba9	82.26	98.92	0.69	82.99	9.14	9.08	92.13	0.68	11.73	3.65
	Ba10	78.12	98.84	0.90	83.54	9.44	8.85	92.98	0.70	11.12	3.65
	Ba11	85.21	99.27	0.48	105.61	12.17	8.68	117.78	0.70	10.57	3.78
	Ba12	79.53	99.13	0.63	96.07	10.96	8.77	107.03	0.67	10.53	3.58
	Ba13	78.19	99.17	0.66	110.66	13.3	8.32	123.96	0.67	10.52	3.59
	Ba14	77.11	98.69	0.98	76.27	8.59	8.88	84.86	0.67	11.05	3.41
	Ba15	80.71	99.11	0.67	95.06	11	8.64	106.06	0.70	10.99	3.59
	Ave.	79.82	98.97	0.85	105.3	11.87	8.87	117.17	0.68	10.76	3.65

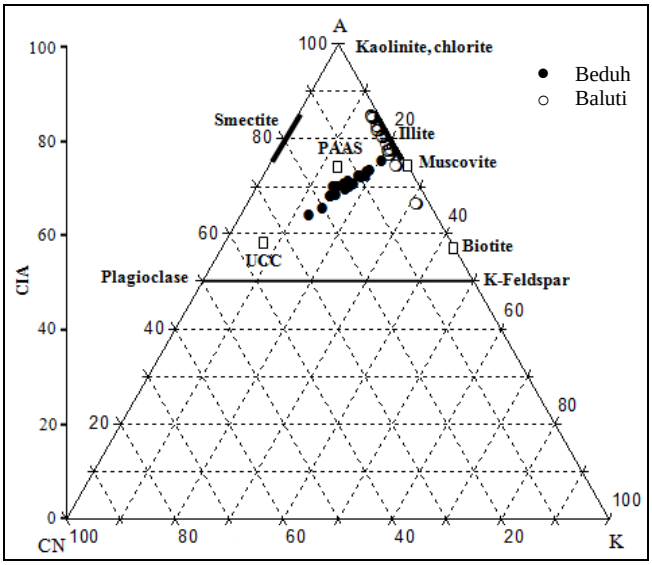

Fig. 7: A-CN-K diagram in molecular proportions for the Beduh and Baluti shales (after Nesbitt and Young, 1984); also plotted is the average Upper Continental Crust and Post Archean Australian Shale (Taylor and McLennan, 1985)

Harnois (1988) proposed the CIW index to monitor paleoweathering at the source area. The Beduh shale possesses CIW average values 91.41 similar to the PAAS value (90.56; Table 5), and 98.97 for Baluti higher than PAAS.

The ICV is useful to estimate the chemical weathering degree (Cox *et al.*, 1995), which illustrates the development of aluminous clay minerals over the silicate minerals. Moreover, the sediments with ICV> 1 are immature with the first cycle of sediments that deposited in active tectonic setting. While, those of ICV< 1, are mature and deposited in a quiescent tectonic environment (Weaver, 1989; Cox *et al.*, 1995). The average of ICV values for the Beduh shale is 1.07 and for Baluti is 0.85 (Table 5). According to the average ICV values, it can be interpreted that the shale of the Beduh Formation is compositionally immature and tectonically affected by active setting; whereas, for Baluti is mature and deposited in quiescent tectonic environment. Thus, the variation in ICV values may be due to the diversity in source-rock composition and in the degree of weathering (Potter *et al.*, 2005).

Provenance

The chemical composition of clastic sedimentary rocks can be attribute to the composition of their source rocks (e.g., Madhavaraju and Lee, 2009; Nagarajan *et al.*, 2011; Armstrong-Altrin, 2014; Awadh and Al-Ankaz, 2016). In order to imply the provenance of clastic rocks, different discrimination diagrams based on major, trace, and rare earth elements, have been proposed by several authors (Floyd *et al.* 1989, 1990; McLennan *et al.*, 1993; Mortazavi *et al.*, 2014).

In the provenance discrimination (TiO_2-Ni bivariate) diagram of Floyd *et al.* (1989), the Beduh and Baluti shales plot in the field of acidic rocks, and the latter are toward more mature (Fig. 8a). However, these study shales are plot in the field of mixed felsic and intermediate rocks on the bivariate diagrams La/Th versus Hf and K_2O versus Rb that proposed by Floyd and Leveridge (1987) as shown in Fig. 8b and c.

The Al_2O_3/TiO_2 ratio in clastic rocks is used to determine the source rock compositions, because this ratio increases from 3 to 8 for mafic rocks, 8 to 21 for intermediate rocks, and 21 to 70 for felsic igneous rocks (Hayashi *et al.*, 1997). The values of the Al_2O_3/TiO_2 ratio for Beduh and Baluti shales are ranged from 16.50 to 28.88 and from 17.81 to 38.86, respectively (Table 6). Cullers (1994) proposed that sediments with Cr/Th ratios ranging from 2.5 to 17.5 and Eu/Eu* values from 0.48 to

0.78 are indicative of felsic sources. The values of the Cr/Th and Eu/Eu* in the Beduh and Baluti samples (3.38 and 0.73 and 9.37 and 0.68, respectively; Tables 5 and 6) generally are within the felsic range. The Cr/Th values (Table 6) indicate the Beduh shale are derived from more acidic source rocks relative to Baluti shale, UCC, and PAAS.

Additionally, the REE patterns can also be used for suggesting the sediment sources, meanwhile felsic rocks have high LREE/HREE ratios and negative Eu anomalies, whereas mafic rocks usually contain low LREE/HREE ratios and no Eu anomalies (e.g., Cullers and Graf, 1983; Cullers, 1994; Absar *et al.*, 2009; Absar and Sreenivas, 2015). The high LREE/HREE (for Beduh and Baluti shales are 8.54 and 8.87, respectively; Table 5) and flat HREE patterns are similar to the PAAS, UCC (Fig. 6), and Precambrian Shield of the Arabian-Nubian Plate (Gebreyohannes, 2014), which indicates a felsic source for the both shales. Accordingly, the felsic igneous rocks are suggested as source rocks for the Beduh and Baluti shales as well as they are slightly influenced by intermediate rocks.

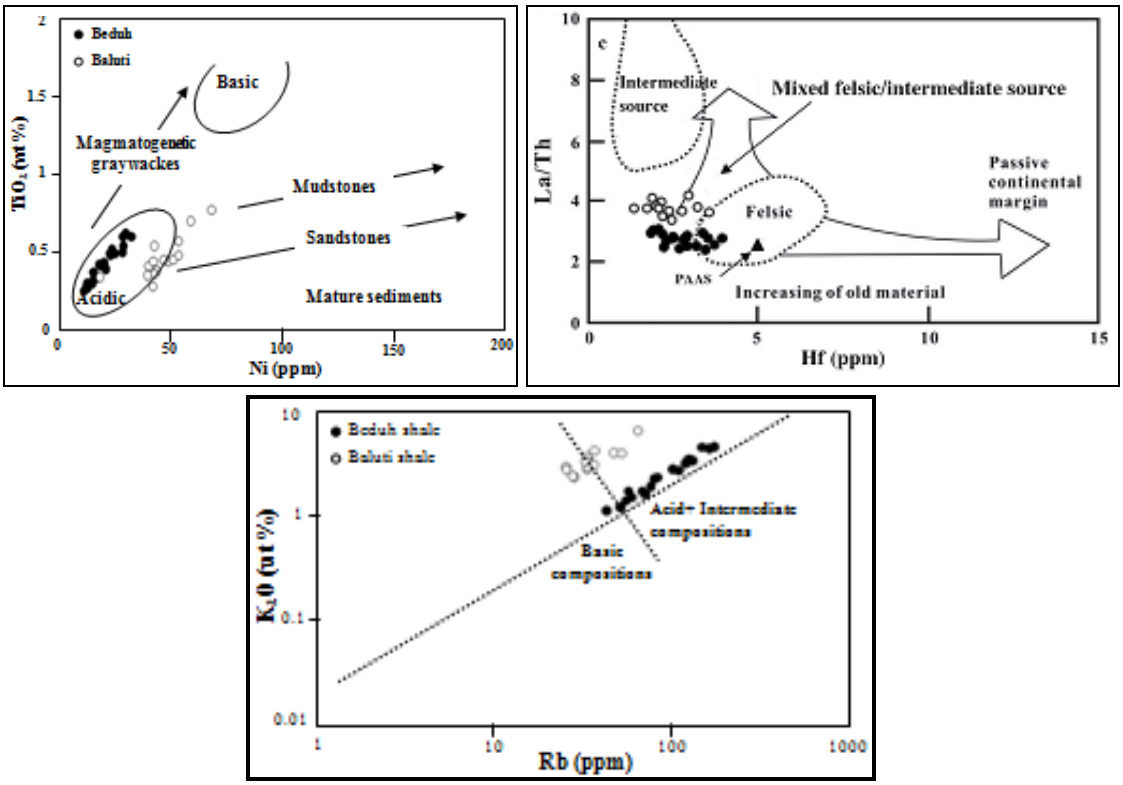

Fig. 8: Provenance discrimination diagrams: a) TiO_2 vs. Ni (after Floyd *et al.*, 1989), b) La/Th vs. Hf (after Floyd and Leveridge, 1987), c) K_2O vs. Rb (after Floyd and Leveridge, 1987)

Table 6: Major and trace element ratios for the shales of the Beduh and Baluti formations

		SiO_2/Al_2O_3	Al_2O_3/TiO_2	K_2O/Na_2O	K_2O/Al_2O_3	Cr/Th	Ni/Co	U/Th	V/V+Ni	V/Cr
Beduh Formation	Be1	3.03	28.08	6.80	0.24	2.74	2.35	0.19	0.81	2.05
	Be2	3.20	24.08	2.33	0.20	3.29	1.91	0.29	0.79	2.19
	Be3	2.96	28.88	4.45	0.23	2.99	1.97	0.19	0.77	2.89
	Be4	2.96	28.40	4.16	0.23	3.35	1.90	0.23	0.79	3.00
	Be5	4.03	24.33	4.06	0.23	2.49	1.77	0.26	0.79	1.87
	Be6	2.90	27.36	6.41	0.24	5.22	1.74	0.22	0.77	2.09
	Be7	3.14	25.40	3.75	0.22	4.77	1.96	0.26	0.77	1.42
	Be8	3.08	26.21	4.83	0.24	3.90	1.96	0.20	0.77	1.49
	Be9	5.24	16.50	1.70	0.20	3.33	1.91	0.28	0.79	0.73
	Be10	2.86	26.98	5.64	0.23	3.92	2.41	0.31	0.78	0.87
	Be11	3.18	23.92	3.19	0.21	2.70	2.21	0.33	0.75	1.15
	Be12	2.82	27.70	9.08	0.25	4.22	2.32	0.19	0.78	3.00
	Be13	3.86	22.44	2.12	0.19	2.92	2.03	0.35	0.78	1.22
	Be14	3.00	26.14	6.16	0.24	3.37	2.11	0.22	0.78	3.11
	Be15	3.01	26.14	6.00	0.23	3.27	2.15	0.23	0.76	2.50
	Be16	3.23	23.78	3.04	0.21	2.19	2.02	0.35	0.78	1.25
	Be17	3.36	21.55	3.38	0.21	2.56	2.46	0.21	0.76	1.49
	Be18	3.97	19.53	1.91	0.20	3.26	1.80	0.38	0.81	1.53
	Be19	3.22	24.16	4.47	0.23	5.65	2.26	0.25	0.76	2.18
	Be20	3.55	22.55	3.01	0.22	3.91	2.53	0.26	0.75	2.12
	Be21	3.20	22.82	3.61	0.23	2.97	2.40	0.17	0.77	2.31
	Averag	3.32	24.62	4.29	0.22	3.48	2.10	0.26	0.78	1.93
Baluti Formation	Ba1	0.81	29.81	40.38	0.25	9.47	6.27	0.40	0.72	1.85
	Ba2	0.60	30.89	36.75	0.21	8.23	5.76	0.50	0.73	2.20
	Ba3	1.43	17.81	34.36	0.29	7.78	6.14	0.33	0.75	2.50
	Ba4	0.57	30.47	36.13	0.16	7.56	6.36	0.39	0.74	2.54
	Ba5	0.54	29.98	27.75	0.19	15.0	6.72	0.50	0.70	1.26
	Ba6	0.48	30.30	34.00	0.16	10.4	4.97	0.35	0.73	1.84
	Ba7	0.44	32.13	32.88	0.18	9.83	7.53	0.46	0.70	2.02
	Ba8	0.80	38.86	38.13	0.44	7.27	3.03	0.82	0.73	1.50
	Ba9	0.67	31.66	28.38	0.19	10.0	7.94	0.55	0.73	2.22
	Ba10	0.43	30.27	34.63	0.25	10.6	7.65	0.54	0.72	1.94
	Ba11	0.52	32.05	34.38	0.15	9.13	5.75	0.42	0.78	2.37
	Ba12	0.34	31.77	42.75	0.23	9.14	7.78	0.51	0.71	2.32
	Ba13	0.54	31.52	49.13	0.25	8.36	5.28	0.50	0.72	2.48
	Ba14	0.60	33.17	32.50	0.26	10.0	9.18	0.63	0.69	2.07
	Ba15	0.79	31.21	38.88	0.21	9.02	7.97	0.57	0.73	2.24
	Averag	0.64	30.79	36.07	0.23	9.46	6.56	0.50	0.73	2.09
PAAS		3.32	19.00	3.09	0.20	7.53	2.39	4.76	0.75	1.71
UCC		4.34	30.40	0.87	0.22	7.76	2.00	3.82	0.71	1.36

Tectonic setting

Various discrimination diagrams, based on the content of major elements in the clastic sediments, are widely employed to determine the tectonic setting of the basins (Bhatia, 1983; Roser and Korsch, 1986). Although several studies proposed that the results inferred from these diagrams were not confirm with the geology of the areas (Valloni and Maynard, 1981; Dostal and Keppie, 2009). The use of these discrimination diagrams has been prudence against by many researchers (e.g., Armstrong-Altrin and Verma, 2005; Ryan and Williams, 2007; Armstrong-Altrin, 2015; Verma and Armstrong-Altrin, 2016).

Recently, Verma and Armstrong-Altrin (2013) suggest two discriminant diagrams, based on the content of major elements, for the tectonic discrimination of clastic

sediments from three main tectonic settings: island or continental arc, continental rift, and collision, originated for the tectonic discrimination of high-silica [$(SiO_2)_{adj}$ = 63% – 95%] and low-silica [$(SiO_2)_{adj}$ = 35% – 63%] types. In addition, Armstrong-Altrin (2015) evaluated these two tectonic diagrams and advice that the two multidimensional diagrams can be considered as a tool for discrimination of the tectonic setting of the old basins. These diagrams were successfully used in recent studies to discriminate the tectonic setting of a source area based on the composition of the clastic sediments (Nagarajan *et al.*, 2015; Tawfik *et al.*, 2015; Zaid *et al.*, 2015).

These diagrams based on the major element compositions were used in this study to determine the tectonic environment of the Beduh and Baluti shales. On the low-silica multidimensional diagram (Fig. 9), most of the Beduh and Baluti shales were plotted in the rift field, which are conform with the geology of the Arabian Shield and the Rutba Uplift (Jassim and Goff, 2006) and some of the Beduh samples fall in collision field, that reveal the possibility that the Beduh shales may consist of sediments derived from active regions of the Mid-Oceanic Ridge to the northeast of Arabian Plate (Fig. 3). In addition it is suggested that the Beduh shale also received sediments by volcanic activity, certitude by the presence of volcaniclastic materials (glass shards and glassy spherules) and smectite as a mixed layer with illite (Hakeem, 2012).

Trace elements especially that are relatively immobile with low residence times in seawater (i.e., La, Nd, Th, Zr, Hf, Nb, and Ti) are assured fingerprints for discrimination of tectonic setting (McLennan *et al.*, 1990; LaMaskin *et al.*, 2008). Several studies have used the REE contents in sediments to identify their plate tectonic settings (e.g., Bhatia and Crook, 1986; McLennan *et al.*, 1990; McLennan and Taylor, 1991; Mader and Neubauer, 2004; Verma and Armstrong-Altrin, 2013). These studies imply the sediments deposited in the continental margin are characterized by LREE enrichment (indicated by high La/Sm) and high total rare earth elements (ΣREE), on the other hand, those from young undifferentiated oceanic arcs have lower La/Sm, lower ΣREE, and lack for Eu anomaly.

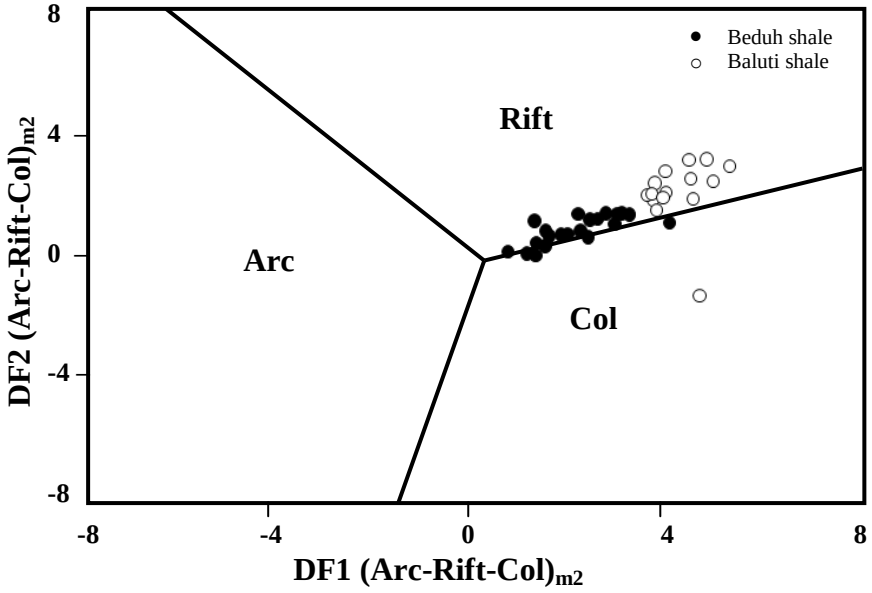

Fig. 9: Discriminant function diagram for low-silica shale samples of the Beduh and Baluti formations (boundaries after Verma and Armstrong-Altrin, 2013)

Discriminant function equations are:

$DF1(Arc\text{-}Rift\text{-}Col)_{m2} = \{0.608 \times In(TiO_2/SiO_2)_{adj}\}+\{-1.854 \times In(Al_2O_3/SiO_2)_{adj}\}+\{0.299\times In(Fe_2O_3t/SiO_2)_{adj}\}+\{-0.550 \times In(MnO/SiO_2)_{adj}\}+\{0.120 \times In(MgO/SiO_2)_{adj}\}+\{0.194 \times In(CaO/SiO_2)_{adj}\}+\{-1.510 \times In(Na_2O/SiO_2)_{adj}\}+\{1.941 \times In(K_2O/SiO_2)_{adj}\}+\{0.003\times In(P_2O_5/SiO_2)_{adj}\}- 0.294.$

$DF2(Arc\text{-}Rift\text{-}Col)_{m2} = \{-0.554 \times In(TiO_2/SiO_2)_{adj}\}+\{-0.995 \times In(Al_2O_3/SiO_2)_{adj}\}+\{1.765 \times In(Fe_2O_3t/SiO_2)_{adj}\}+\{-1.391 \times In(MnO/SiO_2)_{adj}\}+\{-1.034\times In(MgO/SiO_2)_{adj}\}+\{0.225\times In(CaO/SiO_2)_{adj}\}+\{0.713 \times In(Na_2O/SiO_2)_{adj}\}+\{0.330\times In(K_2O/SiO_2)_{adj}\}+\{0.637\times In(P_2O_5/SiO_2)_{adj}\}- 3.631.$

Therefore, the REE patterns of sediments deposited in continental margins can generally be differentiated from those derived from undifferentiated oceanic arcs. Continental margins can be classified into passive and active types. Passive margin provenance is characterized by uniform REE patterns being and similar to PAAS (Bhatia, 1985; McLennan, 1989). Sediments deposited at active continental margins generally show a REE pattern intermediate between a typical andesite pattern and PAAS or in some cases indistinguishable from PAAS itself. Thus, the most active continental margin sediments display intermediate REE abundances, variable LREE enrichments and variable negative Eu anomalies, with Eu/Eu^*_n in the range of 0.6 – 1.0 (McLennan, 1989).

Paleoredox conditions

The redox sensitive elements, such as Cu, Zn, V, Ni, Cr, and U, in the sediments can be used as effective tool for determination of the paleoredox conditions (Jones and Manning, 1994; Madhavaraju and Ramasamy, 1999; Armstrong-Altrin *et al.*, 2015a; Hu *et al.*, 2015).

The U/Th ratio was used as a redox indicator, being higher in organic-rich mudstones (Jones and Manning, 1994). U/Th ratios below 1.25 suggest oxic conditions of deposition, whereas elevated values indicate suboxic and anoxic conditions (Jones and Manning, 1994; Akinyemi *et al.*, 2013). The present study shows a low U/Th ratio (0.17- 0.38, average = 0.24, for the Beduh shale; and 0.33 – 0.82, average= 0.47, for Baluti shale (Table 6), indicating deposition in an oxic environment.

Jones and Manning (1994) and Rimmer (2004) used the elemental ratios (Ni/Co and V/Cr) to deduce the redox conditions during the deposition of the shale. The higher Ni/Co and V/Cr ratios are related to low oxygen levels during the deposition. Jones and Manning (1994) and Sari and Koca (2012) suggested that Ni/Co ratios below 5 indicate oxic environments, whereas ratios of 5 – 7 indicate dysoxic environments and ratios above 7 suboxic to anoxic. The Beduh shale shows a lower Ni/Co ratio (1.74 – 2.53, average = 2.10 nearly similar to the UCC and PAAS; Table 6) suggests an oxic environment, and for Baluti shale (3.03 – 9.18, average = 6.56) reflect the dysoxic depositional environment during deposition of sediments. Jones and Manning (1994) and Armstrong-Altrin *et al.* (2015a) used the V/Cr ratio to infer the depositional environment. A V/Cr ratio below 2 refers to oxic, 2.0 – 4.25 to dysoxic, and higher than 4.25 to suboxic to anoxic conditions. V/Cr ratios of the study shales vary from 0.73 to 3.11 with an average ratio value of 1.93 for Beduh; and 1.26 to 2.54 with an average of 2.09 for Baluti which are higher than for UCC and PAAS (Table 6), indicating an oxic condition during deposition.

CONCLUSIONS

1. The clay mineralogy reveals the tropical to sub-tropical climate during the Lower and Upper Triassic.
2. The study shales show high CaO content (due to the high carbonate content), which have dilution effect on the other oxides and trace elements.

3. The mineralogical and geochemical parameters like illite crystallinity, CIA and CIW values, and A-CN-K diagram reveal moderate to intense for Beduh shale and intensive chemical weathering in the source area for Baluti shale.
4. Major, trace, rare earth elements and elemental ratios imply the felsic and intermediate source rocks for the shales of the Beduh and Baluti, probably from the plutonic-metamorphic complex of the Arabian Shield and Rutba Uplift to the southwest of the basin.
5. The tectonic setting discrimination diagram reveals passive tectonic environment for the study shales with influence of volcanic activity on the Beduh shale.
6. The U/Th, V/Cr, and Ni/Co ratios and negative Eu anomaly (Eu/Eu^*_n) suggest the deposition of the shales under an oxic environment.

REFRENCES

Absar, N., Raza, M., Roy, M., Naqvi, S.M. and Roy, A.K., 2009. Composition and weathering conditions of Paleoproterozoic upper crust of Bundelkhand craton, Central India: records from geochemistry of clastic sediments of 1.9 Ga Gwalior Group. Precamb Res, 168: 313 – 329.

Absar, N. and Sreenivas, B., 2015. Petrology and geochemistry of greywackes of the ~1.6 Ga middle Aravalli Supergroup, Northwest India: evidence for active margin processes. Int Geol Rev, 57: 134 – 158.

Akinyemi, S.A., Adebayo, O.F., Ojo, O.A., Fadipe, O.A. and Gitari, W.M., 2013. Mineralogy and geochemical appraisal of paleo-redox indicators in Maastrichtian outcrop shales of Mamu formation, Anambra Basin, Nigeria. J Natur Sci Res, 3: 48 – 64.

Armstrong-Altrin, J.S., 2015. Evaluation of two multidimensional discrimination diagrams from beach and deep-sea sediments from the Gulf of Mexico and their application to Precambrian clastic sedimentary rocks. Int Geol Rev, 57(11 and 12): 1446 – 1461.

Armstrong-Altrin, J.S., Lee, Y.I., Kasper-Zubillaga, J.J., Carranza-Edwards, A., Garcia, D., Eby, N., Balaram, V. and Cruz-Ortiz, N.L., 2012. Geochemistry of beach sands along the western Gulf of Mexico, Mexico: implication for provenance. Chem Erde Geochem, 72: 345 – 362.

Armstrong-Altrin, J.S., Machain-Castillo, M.L., Rosales-Hoz, L., Carranza-Edwards, A., Sanchez-Cabeza, J. and Ruiz-Fernandez, A.C., 2015. Provenance and depositional history of continental slope sediments in the Southwestern Gulf of Mexico unraveled by geochemical analysis. Continental Shelf Res, 95: 15 – 26.

Armstrong-Altrin, J.S., Nagarajan, R., Lee, Y.I., Kasper-Zubillaga, J.J. and Córdoba-Saldaña, L.P., 2014. Geochemistry of sands along the San Nicolás and San Carlos beaches, gulf of California, Mexico: implication for provenance. Turk J Earth Sci, 23: 533 – 558.

Armstrong-Altrin, J.S. and Verma, S.P., 2005. Critical evaluation of six tectonic setting discrimination diagrams using geochemical data of Neogene sediments from known tectonic setting. Sed Geol, 177: 115 – 129.

Awadh, S.M. and Al-Ankaz, Z.S., 2016. Geochemistry and petrology of Late Miocene-Pleistocene Dibdibba sandstone formation in south and central Iraq: implications for provenance and depositional setting. Arab Jour Geosc, 9: 526 – 540.

Bellen, R.C., Dunnington, H.V., Wetzel, R. and Morton, D., 1959. Lexique Stratigraphique Internal Asie. Iraq. International Geological Congress. Comm. Stratigr. 3, Fasc. 10a, 333p.

Bhatia, M.R., 1983. Plate tectonics and geochemical composition of sandstones. J Geol, 91: 611– 627.

Bhatia, M.R., 1985. Rare earth element geochemistry of Australian Paleozoic graywackes and mud rocks: provenance and tectonic control. Sed Geo, 45: 97 – 113.

Bhatia, M.R. and Crook, K.A.W., 1986. Trace element characteristics of greywackes and tectonic setting discrimination of sedimentary basins. Contrib Mineral Petrol, 92: 181 – 193.

Carroll, D., 1970. Clay minerals: a guide to their x-ray identification. Geol Soc Am, 80p.

Chamley, H., 1989. Clay sedimentology. Springer Verlag, Berlin and New York.

Condie, K.C., 1991. Another look at rare earth elements in shales. Geochim Cosmochim Acta, 55: 2527 – 2531.

Cox, R., Lowe, D.R. and Cullers, R.L., 1995. The influence of sediment recycling and basement composition on evolution of mudrock chemistry in the southwestern United States. Geochim Cosmochim Acta, 59(14): 2919 – 2940.

Cullers, R.L., 1994. The controls on major and trace element variation of shales, siltstones, and sandstones of Pennsylvanian-Permian age from uplifted continental blocks in Colorado to platform sediment in Kansas, USA. Geochim Cosmochim Acta, 58: 4955 – 4972.

Cullers, R.L. and Graf, J., 1983. Rare earth elements in igneous rocks of the continental crust: intermediate and silicic rocks, ore petrogenesis. In: Henderson, P., (ed), Rare-Earth Geochemistry. Amsterdam, the Netherlands: Elsevier, 275 – 312.

Dai, S., Graham, I.T. and Ward, C.R., 2016. A review of anomalous rare earth elements and yttrium in coal. Int J Coal Geol, 159: 82 – 95.

Dostal, J. and Keppie, J.D., 2009. Geochemistry of low-grade clastic rocks in the Acatlan Complex of southern Mexico: evidence for local provenance in felsic-intermediate igneous rocks. Sediment Geol, 222: 241 – 253.

Fedo, C.M., Eriksson, K. and Krogstad, E.J., 1996. Geochemistry of shale from the Archean (~3.0 Ga) Buhwa Greenstone belt, Zimbabwe: implications for provenance and source area weathering. Geochim Cosmochim Acta, 60: 1751 - 1763.

Fedo, C.M., Nesbitt, H.W. and Young, G.M., 1995. Unraveling the effects of potassium metasomatism in sedimentary rocks and paleosols, with implications for paleoweathering conditions and provenance. Geology, 23: 921 – 924.

Floyd, P.A., Franke, W., Shail, R. and Dorr, W., 1990. Provenance and depositional environment of Rhenohercynian synorogenic greywacke from the Giessen nappe, Germany. Geologische Rundschau, 79: 611– 626.

Floyd, P.A. and Leveridge, B.E., 1987. Tectonic environment of the Devonian Gramscatho basin, South Cornwall: framework mode and geochemical evidence from turbiditic sandstones. J Geol Soci London, 144: 531 –542.

Floyd, P.A., Winchester, J.A. and Park, R.G., 1989. Geochemistry and tectonic setting discrimination using immobile elements. Earth Planet Sci Lett, 27: 211 – 218.

Gebreyohannes, G.W., 2014. Geology, geochemistry and geochronology of Neoproterozoic rocks in western Shire, Northern Ethiopia. MSc, University of Oslo, Oslo, Norway.

Ghandour, I.M., Masuda, H. and Maejima, W., 2003. Mineralogical and chemical characteristics of Bajocian-Bathonian shales, G. Al-Maghara, North Sinai, Egypt: climatic and environmental significance. Geochem J, 37: 87 – 108.

Hakeem, F.A., 2012. Sedimentology and suitability for some ceramic industries of Beduh Formation (Lower Triassic), Northern Thrust Zone, Kurdistan Region. PhD, Salahaddin University, Erbil, Iraq.

Hallam, A., Grose, J.A. and Ruffell, A.H., 1991. Paleoclimatic significance of changes in clay mineralogy across the Jurassic- Cretaceous boundary in England and France. Palaeogeog Palaeoclimat Palaeoecol, 81: 173 –187.

Hanna, M.T., 2007. Palynology of the upper part of Baluti Formation (Upper Triassic) and the nature of its contact with the Sarki Formation (Lower Jurassic) at Amadiya district, Northern Iraq. PhD, Mosul University, 143p.

Harnois, L., 1988. The CIW index: a new chemical index of weathering. Sediment Geol, 55: 319 – 322.

Hayashi, K., Fujisawa, H., Holland, H.D. and Ohmoto, H., 1997. Geochemistry of ~1.9 Ga sedimentary rocks from northeastern Labrador, Canada. Geochim Cosmochim Acta, 61: 4115 – 4137.

Hu, J., Li., Q., Huang, J. and Ge, D., 2015. Geochemical characteristics and depositional environment of the middle Permian mudstones from central Qiangtang Basin, northern Tibet. Geol J, doi:10.1002/gj.2653.

Jassim, S.Z., Buday, T. and Cicha, I., 2006. Tectonic framework. In: Jassim, S.Z. and Goff, J.C. (eds), Geology of Iraq. Prague, Czech Republic: Dolin, 45 – 56.

Jassim, S.Z. and Goff, J.C., 2006. Phanerozoic development of the Northern Arabian Plate. In: Jassim, S.Z. and Goff, J.C. (eds), Geology of Iraq. Prague, Czech Republic: Dolin, 15 – 34.

Jones, B. and Manning, D.A.C., 1994. Comparison of geochemical indices used for the interpretation of paleoredox conditions in ancient mudstones. Chem Geol, 111: 111 – 129.

LaMaskin, T.A., Dorsey, R. and Vervoort, J.D., 2008. Tectonic controls on mudrock geochemistry, Mesozoic rocks of eastern Oregon and western Idaho, USA: implications for cordilleran tectonics. J Sed Res, 78(12): 765 – 783.

Mader, D. and Neubauer, F., 2004. Provenance of Paleozoic sandstones from the Carnic alps (Austria): petrographic and geochemical indicators. Inter J Earth Sci, 93: 262 – 281.

Madhavaraju, J. and Lee, Y.I., 2009. Geochemistry of the Dalmiapuram Formation of the Uttatur Group (Early Cretaceous), Cauvery basin, southeastern India: Implications on provenance and paleo-redox conditions. Rev Mexi Cie Geol, 26(2): 380 – 394.

Madhavaraju, J. and Ramasamy, S., 1999. Rare earth elements in limestones of Kallankurich-chi Formation of Ariyalur Group, Tiruchirapalli Cretaceous, Tamil Nadu. J Geol Soc India, 54: 291 – 301.

Maynard, J.B., 1992. Chemistry of modern soils as a guide to interpreting Precambrian paleosols. J Geol, 100: 279 – 289.

McLennan, S., Hemming, S., McDaniel, D. and Hanson, G., 1993. Geochemical approaches to sedimentation, provenance, and tectonics. Geol. Soc. Am Spec Pap, 284: 21 – 40.

McLennan, S.M., 1989 Rare earth elements in sedimentary rocks: influence of provenance and sedimentary processes. Rev Miner Geochem, 21:169 – 200.

McLennan, S.M. and Taylor, S.R., 1991. Sedimentary rocks and crustal evolution: tectonic setting and secular trends. J. Geol., 99: 1 – 21.

McLennan, S.M., Taylor, S.R., Mcculloch, M.T. and Maynard, J.B., 1990. Geochemical and Nd-Sr isotopic composition of deep-sea turbidites: crustal evolution and plate tectonic associations. Geochim Cosmochim Acta, 54: 2015 – 2050.

Merriman, R.J. and Frey, M., 1999. Patterns of very low-grade metamorphism in metapelitic rocks. In: FreyM, Robinson D (eds) Low-grade metamorphism. Blackwell Science, Oxford, 61 – 107.

Mortazavi, M., Moussavi-Harami, R., Mahboubi, A. and Nadjafi, M., 2014. Geochemistry of the Late Jurassic–Early Cretaceous shales (Shurijeh Formation) in the intracontinental Kopet-Dagh Basin, northeastern Iran: implication for provenance, source weathering, and paleoenvironments. Arab J Geosci, 7: 5353 – 5366.

Nagarajan, R., Armstrong-Altrin, J.S., Kessler, F.L., Hidalgo-Moral, E.I., Dodge-Wan, D. and Taib, N.I., 2015. Provenance and tectonic setting of Miocene siliclastic sediments, Sibuti Formation, northwestern Borneo. Arab J Geosci, 8: 8549 – 8565.

Nagarajan, R., Madhavaraju, J., Nagendra, R., Armstrong-Altrin, J.S. and Moutte, J., 2011. Geochemistry of Neoproterozoic shales of the Rabanpalli Formation Bhima Basin, Northern Karnataka, southern India: implications for provenance and paleoredox conditions. Rev Mex Cien Geol, 24: 20 – 30.

Nagarajan, R., Madhavaraju, J., Nagendra, R., Armstrong-Altrin, J.S. and Moutte, J., 2007. Geochemistry of Neoproterozoic shales of the Rabanpalli formation, Bhima Basin, northern Karnataka, southern India: implications for provenance and paleoredox conditions. Rev Mexi Cie Geol, 24: 150 – 160.

Nesbitt, H.W., Fedo, C.M. and Young, G.M., 1997. Quartz and feldspar stability, steady and non-steady state weathering and petrogenesis of siliciclastic sands and muds. J Geol, 105: 173 – 191.

Nesbitt, H.W. and Young, G.M., 1984. Prediction of some weathering trends of plutonic and volcanic rocks based on thermodynamic and kinetic considerations. Geochim Cosmochim Acta, 48: 1523 – 1534.

Nesbitt, H.W. and Young, G.M., (1996). Petrogenesis of sediments in the absence of chemical weathering: effects of abrasion and sorting on bulk composition and mineralogy. Sediment, 43: 341 – 358.

Nesbitt, H.W. and Young, G.M., 1982. Early Proterozoic climates and plate motions inferred from major element chemistry of lutites. Nature, 299: 715 –717

Numan, N.M.S., 1997. A plate tectonic scenario for the Phanerozoic succession in Iraq. Iraqi Geol. J., 30: 1 – 28.

Oliveira, A., Rocha, F., Rodrigues, A., Jouanneau, J.M., Dias, A., Weber, O. and Gomes, C., 2002. Clay minerals from the sedimentary cover from Northwest Iberian Shelf. Prog Ocean, 52: 233 – 247.

Potter, P.E., Maynard, J.B. and Depetris, P.J., 2005. Mud and mudstones: introduction and overview. Springer-Verlag, New York.

Raucsik, B. and Merényi, L., 2000. Origin and environmental significance of clay minerals in the lower Jurassic formations of the Mecsek Mts., Hungary. Acta geol. Hungarica, 43: 405 – 429.

Rimmer, S.M., 2004. Geochemical paleoredox indicators in Devonian-Mississippian black shales, Central Appalachian Basin (USA). Chem Geol, 206: 373 – 391.

Roser, B.P. and Korsch, R.J., 1986. Determination of tectonic setting of sandstone-mudstone suites using SiO_2 content and K_2O/Na_2O ratio. J. Geol., 94: 635 – 650.

Ryan, K.M. and Williams, D.M., 2007. Testing the reliability of discrimination diagrams for determining the tectonic depositional environment of ancient sedimentary basins. Chem Geol, 242: 103 – 125.

Sari, A. and Koca, D., 2012. An approach to provenance, tectonic and redox conditions of Jurassic-Cretaceous Akkuyu Formation, Central Taurids, Turkey. Mineral Res Explor Bull, 144: 51 – 74.

Sheldon, N.D., 2003. Pedogenesis and geochemical alteration of the picture gorge subgroup, Columbia River basalt, Oregon. Geol Soc Am Bull, 115: 1377 – 1387.

Sissakian, V.K., 2000. Geological map of Iraq (scale 1:1000000, sheet no.1, 3rd edition). GEOSURV, Baghdad.

Srivastava, A.K., Randive, K.R. and Khare, N., 2013. Mineralogical and geochemical studies of glacial sediments from Schirmacher oasis, East Antarctica. Quarter Int, 292: 205 – 216.

Tawfik, H.A., Ghandour, I.M., Maejima, W. and Abdel-Hameed, A.T., 2011. Petrography and geochemistry of the lower Paleozoic Araba formation, northern Eastern Desert, Egypt: implications for provenance, tectonic setting and weathering signature. J Geosci Osaka, 54: 1 – 16.

Tawfik, H.A., Ghandour, I.M., Maejima, W., Armstron-Altrin, J.S. and Abdel- Hameed, A.T., 2015. Petrography and geochemistry of the siliciclastic Araba Formation (Cambrian), east Sinai, Egypt: implications for provenance, tectonic setting and source weathering. Geol Mag, doi.org/10.1017/S0016756815000771.

Taylor, S.R. and McLennan, S.H., 1985. The geochemical evolution of the continental crust. Rev Geophys, 33: 241 – 265.

Valloni, R. and Maynard, B., 1981. Detrital modes of recent deep-sea sands and their relation to tectonic setting: a first approximation. Sediment, 28: 75 – 83.

Verma, S.P. and Armstrong-Altrin, J.S., 2013. New multi-dimensional diagrams for tectonic discrimination of siliclastic sediments and their application to Precambrian basins. Chem Geol, 355: 117 – 133.

Verma, S.P. and Armstrong-Altrin, J.S., 2016. Geochemical discrimination of siliclastic sediments from active and passive margin settings. Sediment Geol, 332: 1 –12.

Weaver, C.E., 1989. Clays, muds, shales. Developments in sedimentology. Elsevier, Amsterdam.

Zaid, S.M., Elbadry, O., Ramadan, F. and Mohamed, M., 2015. Petrography and geochemistry of Pharaonic sandstone monuments in tall san Al Hagr, Al Sharqiya governorate, Egypt: implications for provenance and tectonic setting. Turk J Earth Sci, 24: 344 – 364.